

# Experimental study of fabricating SiC mirror in full aperture with optimized fixed abrasive polishing pad

Xu Wang (王旭)\* and Feng Zhang (张峰)

Key Laboratory of Optical System Advanced Manufacturing Technology, Changchun  
Laboratory of Optics, Fine Mechanics and Physics, Chinese Academy of Science,  
Changchun 130033, China

\*Corresponding author: 13844848195@163.com

Received August 2, 2013; accepted September 30, 2013; posted online March 20, 2014

The removal function test is carried out on the earlier round-pellet polishing pad. The concept of filling factor is introduced to evaluate the removal function obtained from the experiments mentioned in the paper. To improve the filling factor and characteristics of the polishing pad, the pad structure is optimized according to the experimental results of the round-pellet pad. The removal function of the new polishing pad is simulated with MATLAB. The stability experiment is carried out in full aperture at the same time. The fixed abrasive and the slurry abrasive polishing experiment both are performed under the same conditions. Finally, the structural similarity index is introduced to evaluate the similarity between simulations and experiments. The best structural similarity index of multi-square-pellet pad is 0.4257. The comparison results are acceptable and positive. The optimized fixed abrasive polishing pad is proved to be highly promising for large-diameter SiC mirror fabrication.

OCIS codes: 220.0220, 220.4000, 220.4610, 220.5450.  
doi: 10.3788/COL201412.S12203.

New-generation ground observing system needs to own higher ground-resolving power and wider swatch, which demands large diameter, off-axis and higher light. The optical mirror with large diameter is the key component of the optical remote imaging. So, fabricating the optical mirror with the characteristics mentioned above is the most important task.

As the Reaction Bonded SiC has extremely high rigidity and stability, it is the perfect material for fabricating large-diameter mirror<sup>[1]</sup>. However, its good characteristic becomes the biggest drawback in fabrication. So, due to its high stiffness, SiC mirror fabrication will not be an easy job.

Fabricating SiC mirror with slurry is a traditional, but advanced method. The method of fabricating hard brittle material with slurry has been researched in microstructure decades ago, especially in the mechanism and in critical condition from brittle removal to plastic removal<sup>[2,3]</sup>. Owing to the fabrication circumstance effects, the traditional slurry technology causes the unstable fabrication accuracy, low efficiency and high-fabrication cost.

Compared with slurry, the fixed abrasive technology is able to solve the mentioned problems. The fixed abrasive technology developed in 1970s can offer several potential advantages over the slurry process with pitch or polyurethane laps. These advantages include polishing efficiency, temperature stability, cost of consumables, and compatibility with numerically controlled generating techniques<sup>[4]</sup>. So, the fixed abrasive technology becomes an alternative option to finish the optical mirrors. Edwards and Hed studied in detail the fine grinding mechanism (ductile cutting) using bound diamond abrasives<sup>[5]</sup>. They found that the fracture

mechanism is preferred to plastic scratching for most of the applications. And, the engineers in 3M company commercialize the fixed abrasive technology successfully<sup>[6,7]</sup>. Bifano from Boston University has also proved that it is possible to fabricate high-precision ceramic aspherical mirror using ductile cutting characteristic of the fixed abrasive technology<sup>[8-10]</sup>.

We are expecting that certain amount of the material can be removed at any fabricating spot on the mirror when fabricating the SiC aspherical mirror, which is called the deterministic fabrication. In order to obtain the effect of the deterministic fabrication, the removal function of the fixed abrasive technology becomes our key research point.

In our early experiment<sup>[11,12]</sup>, the specifications of the used pellets are given in Table 1.

The distance of the back-fence pellets is set as 10 mm, the eccentricity is 9 mm, which are optimized in detail in a study conducted by Xu *et al.*<sup>[12]</sup>. The representative result is displayed in Fig.1 and Fig.2.

To evaluate the relationship between theoretical removal function and the experiments, the concept of RMS curve distance is introduced in the paper. Eq. (1) is the formula of the concept:

$$D_{rms} = \|f_1 - f_2\| = \left( (f_1 - f_2)^T (f_1 - f_2) \right)^{1/2}. \quad (1)$$

Based on the data in Fig. 3, the RMS distance between the two curves is  $D_{rms} = 0.0849 \mu\text{m}$ , and the error of the two curves is  $0.0849 \mu\text{m}$ .

In Fig. 1, the minimum absolute value of the experimental removal curve is lower than the theory because break-in ability of the pellets on the pad is less. In the fabrication process, the worn diamond particles in the

**Table 1.** Specifications of pellet

Material	resin
Abrasive	diamond
Pellet concentration (%)	25%
Volume ratio of diamond (%)	6.25%
Pellet stiffness (JB1192-71)	Middle soft
Abrasive diameter ( $\mu\text{m}$ )	5
Pellet diameter (mm)	10
Pellet thickness (mm)	5
Pellet surface type	plane

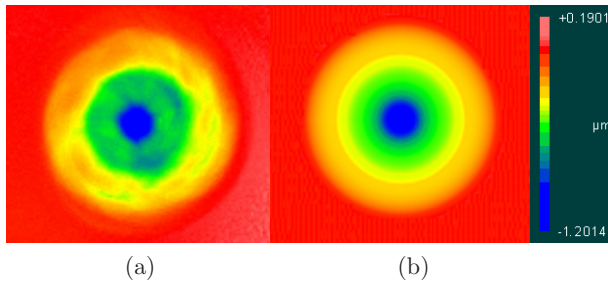


Fig. 1. Surface/wavefront map comparison of (a) experimental removal function and (b) theoretical removal Function.

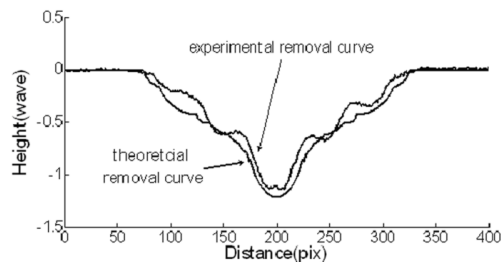


Fig. 2. Generatrix comparison of the theoretical and the experimental removal function.

pellets cannot fall off in time; so, the new diamond particles will not be to join the fabrication, the final result is less than that expected in the theory. For better break-in ability of the pellets, the binding ability of the resin in pellets should be reduced properly, the stiffness of the pellets should also be reduced, which makes the diamond particles fall off in time when the particles are worn. Although the method reduces the utilization of the abrasive, it is obvious that the material removal rate improves evidently.

It is obvious that the curve in Fig. 2 is not smooth enough. The maximum and the minimum exist in the local area, which is called as the “step” effect. We are trying to introduce the filling factor to evaluate the step effect. It is defined as the ratio of the pellet working contact area to envelop of this surface area. The definition is described as Eq. 2.

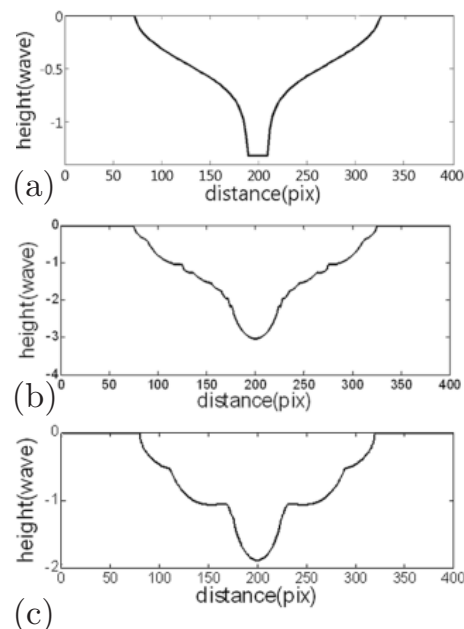
$$\mu = \frac{S_{\text{contact}}}{S_{\text{contour}}}. \quad (2)$$

For example, in the traditional polishing technology, the pitch polishing pad is round, its filling factor is  $\mu = 100\%$  without any grooves on it. According to the distribution of seven pellets, the polishing pad filling factor is  $\mu = 77.78\%$ . But, the filling factor of the polishing pad with four pellets is  $\mu = 68.65\%$ . The simulated removal function of the round pitch pad, 7 pellets pad, 4 pellets pad are displayed in Fig. 3 respectively.

The step effect reflects the spatial frequency error of the polishing pad. The spatial frequency of the pad can be copied onto the mirror surface. So, the inconspicuous step effect is the key factor to obtain a better mirror surface. Improving the filling factor will be an effective method to reduce the step effect.

The round-pellet pad with obvious step effect is used to fabricate an SiC mirror in the experiment. The ripple emerges on the mirror surface clearly. Improving the filling factor is the key method to optimize the working characteristic of the removal function. Our aim is to increase the effective working area of the polishing pad and to make the removal function approach the Gaussian function.

According to the experimental results, the pad with round pellets is not an effective method to improve the filling factor. Improving the contact area between the pellets and the workpiece in unit area is necessary; reducing the interspace among the pellets is a better way. Based on this rule, triangle pellets, square pellets, hexagon pellets are chosen as experiment objects. The next step is to find out which shape pellet is the best. The pads with triangle pellets, square pellets, hexagon pellets are made, the distance between pellets is set at 1 mm. Three types of pellets are used to fabricate the SiC mirror. The experiment results indicate that the

Fig. 3. Relationship between the filling factor and “step” effect. (a) filling factor  $\mu = 100\%$ ; (b) filling factor  $\mu = 77.78\%$ ; (c) filling factor  $\mu = 68.65\%$ .

fabrication results between the pad with triangle pellets and square pellets; the pad with hexagon pellets has a serious worn in the middle and the corresponding area in the mirror. The result is analyzed, which indicates that the pad with hexagon pellets has alveolate structure, which goes against the flowing of the coolant and lubricant. So, the level of worn out on the pad is different. As far as the triangle pellets are concerned, the pellet with triangle structure is difficult to manufacture, which has much more wasters. The manufacture cost is much higher. At the end of the experiment, the pad with square pellets is the most optimized. The comparison of the theory and experiment processes is not the focus of this paper, only the corresponding results are given. The structure of multi-square pellets has some advantages: firstly, the square pellets are manufactured easily, which reduces the fabrication cost. Secondly, if the interspace among the square pellets is optimized, the coolant and lubricant can flow between the pellets easily, which is good to obtain a better mirror surface<sup>[7]</sup>.

For the convenience of simulation, the calculation of the multi-square pellets removal function is divided into two steps:

Firstly, the removal function of the single square pellet is simulated in the planar movement. For the single square pellet in the movement, it is very difficult to calculate the removal function with integral. The discrete method is a better solution. The single square pellet surface is divided into  $n \times n$  matrix points. Then, the movement track of every single point is calculated and analyzed, then, the  $n^2$  points are calculated in the same method. At the end of the calculation, all the movement tracks are superposed, which results in 3D removal function. It is also discrete of course.

Secondly, because of the linear superposition characteristic of the single square pellet removal function, the multi-square pellets removal function can be obtained through superposing of the single square pellet according to its own position on the polishing pad. The obtained discrete removal function should be filtered and smoothed to achieve the final removal function. The calculation results are displayed in Fig. 4.

In the process of the experiment, fabrication parameters such as pellet position, diameter, eccentricity are all set as same in the simulation. The whole experiment is carried out on the CNC system manufactured by our

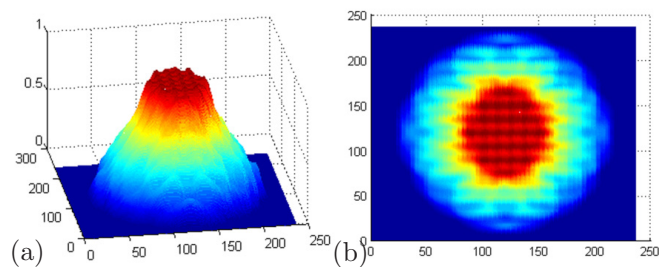


Fig. 4. Simulation removal function of multi-square pellet polishing pad: (a) 3D simulation; (b) 2D simulation.

institute. It has the ability to fabricate 1200 mm work-piece, has 5 axes, locating accuracy is  $5 \mu\text{m}$ , the biggest fabrication pressure is 0.5 MPa, the speed of the fabrication axis is 210 rpm, the eccentricity is 10 mm.

Fig. 5 shows the picture of the multi-square pellets.

An SiC mirror, which can be tested with interferometer, is prepared before the experiment. The surface data are saved firstly; its position and rotating angle are also recorded. The SiC mirror is fabricated at a fixed point in the following experiment.

The workpiece is put at the pre-marked position after the fabrication and tested with interferometer. We can obtain the removal function of the pad through the difference between tests. Fig. 6 shows the experimental and simulated removal function.

By comparing Fig. 1(a) with Fig. 6(a), it was found that after changing the pellet shape, the filling factor improved, the step effect reduced, the profile of the removal function became much smoother.

To test the long-time fabrication stability of the optimized pad, an SiC mirror is fabricated with the multi-square pellet pad. The mirror surface is plane, material used is SiC, as displayed in Fig. 7. The length is 205 mm and width is 125 mm.

The average diameter of diamond particle is  $7 \mu\text{m}$ , the highest pressure is 0.5 MPa, the optimized eccentricity is 9 mm and the rotating speed is 200 r/min.

Experimental steps are follows:

(1) The initial mirror surface is tested with interferometer, the result is saved as DAT file.

(2) The DAT file is used as input into the ASM software(Asphere Surface Manufacture); the mirror size, fabrication tracks, polishing pad diameter, eccen-



Fig. 5. The picture of multi-square pellet polishing pad.

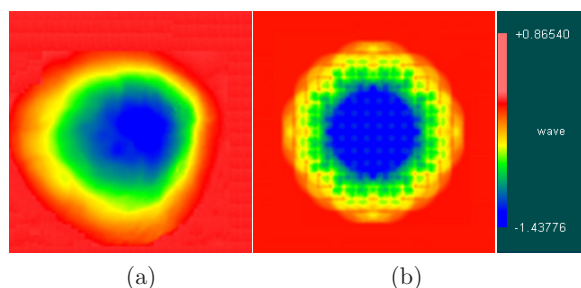


Fig. 6. Removal function picture of multi-square pellet pad: (a) experimental removal function and (b) simulated removal function.

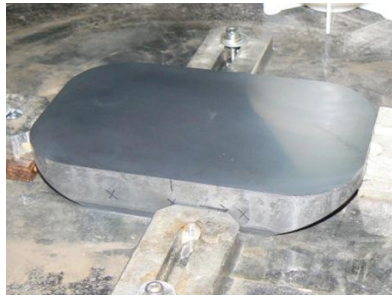


Fig. 7. Picture of SiC mirror.

tricity are used as input into the software. The fabrication controlling file is created by the ASM software<sup>[13,14]</sup>.

(3) The UMAC system is controlled by the fabrication controlling file to fabricate the SiC mirror.

(4) When finishing the fabrication, the removal distribution is obtained with “Subtract Sys Err” function in interferometer software.

(5) In matlab, the idealized removal distribution is created with fabrication controlling file and idealized removal function. The error between the idealized and experimental removal distribution reflects the removal function stability of the multi-square pellet polishing pad.

(6) Step (1) is repeated to gain the next group of data. The step mentioned above tests the long-time stability of the removal function of the multi-square pellet polishing pad.

Some experimental results are obtained according to the steps mentioned above; the pictures displayed in Figs. 8(a), (c) and (e) are the results in different fabrication phases.

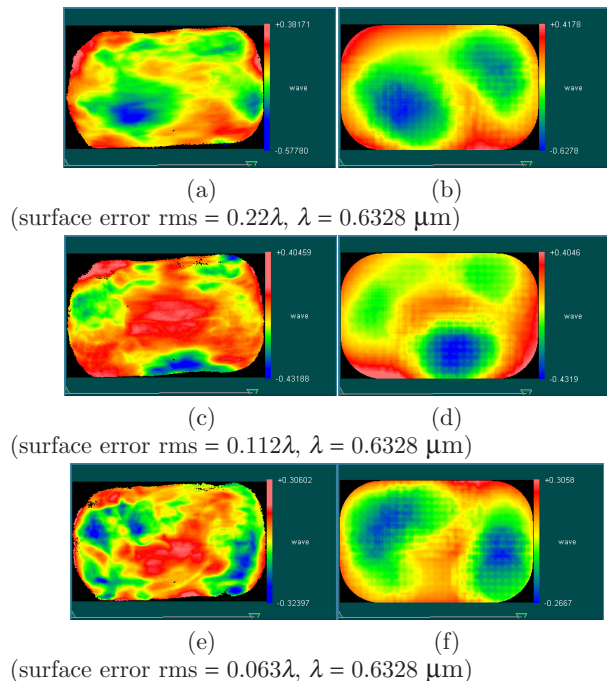


Fig. 8. Removal map of polishing SiC mirror: (a), (c) and (e) measured removal map and (b), (d) and (f) simulation removal map.

The experimental results are analyzed as follows:

(1) The experimental results observed in Fig. 6(a) are not as ideal as Fig. 1(a) because of the large pellet number, almost over 100 pellets. In the fabrication process, the size of diamond particles, concentration, the break-in characteristic of each pellet cannot be same strictly, so the probability of disfigurement is much higher than the pad with seven round pellets. Finally, this leads to the faulty removal function.

(2) As far as the details in Figs. 8(a)–(f) are concerned, the experimental results are not identical with the simulation strictly; however, both are similar in the full aperture. The comparison results indicate that the break-in ability of the multi-square pellets is maintained well in the long-time fabrication. The removal function of the polishing pad is maintained stable easily, which is a very obvious advantage in fabricating the large-diameter SiC mirror.

For intuitionistic comparison, the slurry technology is also used to fabricate the same size SiC mirror under identical conditions. In the slurry fabrication, the additional slurry is not used, whose purpose is to examine the fabrication ability with the same amount of slurry. The experimental steps are identical with the fixed abrasive experiment.

Two representative results are adopted as displayed in Figs. 9(a)–(d).

The distribution in Figs. 9(a) and (b) has good comparability, but the situation in Figs. 9(c) and (d) is not favorable. This difference indicates that although the slurry technique has very high fabrication accuracy, it is difficult to maintain stable long-time fabrication. If we have to maintain the removal function stable, the slurry and water have to be added constantly. The optician must be experienced well in the process of adding the slurry. The perfect ratio of the slurry and water gives a perfect fabrication result. If the slurry is superabundant, the excess abrasives collide, friction each other, which results in the reduction of the effective working particles and fabrication efficiency. On the contrary, if

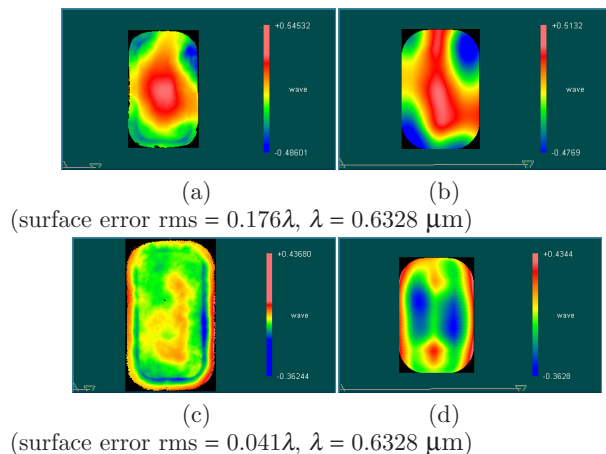


Fig. 9. Removal map of polishing SiC mirror: (a) and (c) measured removal map; (b) and (d) simulation removal map.

the water is superabundant, the slurry gets washed out, which also causes the reduction in the effective working particles. However, these problems do not occur in the fixed abrasive technology.

For quantitative analysis on the fabrication results, the concept of the structure similarity exponent is introduced to evaluate the relationship between simulation and experiment<sup>[15]</sup>. As far as the simulation and experiment results are concerned, the bigger the structure similarity exponent is, the much more similar they are.

The structure similarity exponent equation is as follows:

$$SSIM(x, y) = \frac{(2\mu_x\mu_y + C_1)(2\sigma_{xy} + C_2)}{(\mu_x^2 + \mu_y^2 + C_1)(\sigma_x^2 + \sigma_y^2 + C_2)}, \quad (3)$$

where,  $\mu_x$ ,  $\mu_y$  are the average intensities of the discrete data,  $\sigma_x$ ,  $\sigma_y$  are the standard deviations. The constant  $C_1$  is introduced to avoid the unstable result when  $\mu_x^2 + \mu_y^2$  approaches 0. The constant  $C_2$  is introduced to avoid the unstable result when  $\sigma_x^2 + \sigma_y^2$  approaches 0.  $\sigma_{xy}$  is denoted as:

$$\sigma_{xy} = \frac{1}{N-1} \sum_{i=1}^N (x_i - \mu_x)(y_i - \mu_y). \quad (4)$$

The structure similarity exponent in Figs. 8 and 9 is calculated using Eq. (3). The results are listed in Table 2.

Based on the results in Table 2, the removal function shape of the slurry is unstable, which is affected by the uncontrollable factor of the fabrication circumstance. However, the removal function of the multi-square pellet pad is much more stable, which is obvious in long-time fabrication especially.

In conclusion, the filling factor is introduced to evaluate the removal function of the round-pellet polishing pad. According to the concept of the filling factor, the

**Table 2.** The structural similarity index of surfacing distributing matrix

Fixed abrasive		Slurry abrasive		
Figs. 12(a) and (b)	Figs. 12(c) and (d)	Figs. 12(e) and (f)	Figs. 13(a) and (b)	Figs. 13(c) and (d)
0.4257	0.3512	0.3037	0.4186	0.2514

pellet structure on the pad is optimized. The removal function of the new pad is simulated in Matlab. According to the simulated parameters, the experiment of optimizing the multi-square pellet pad and its actual removal distribution are carried out. The experiment tests the long-time fabrication stability of the new polishing pad. The concept of the structure similarity exponent is introduced to evaluate the simulated and experimental full aperture removal. The final similarity comparison results indicate that the similarity of multi-square pellet is not only higher than slurry, but also much more stable than that. The final results are optimistic, which indicates that the multi-square pellet polishing pad is a promising application foreground in fabrication of the large-diameter SiC mirror.

This work was supported by the 973 national funding of "Study on the basic theory and key techniques of space optical fabrication and metrology" (No. 2011CB01320005).

## References

1. W. J. Choyke, R. F. Farich, and R. A. Hoffman, *Appl. Opt.* **15**, 2006 (1976).
2. D. Golini and S. D. Jacobs, *Appl. Opt.* **30**, 2761 (1991).
3. J. C. Lambropoulos, S. Xu, and T. Fang, *Appl. Opt.* **36**, 1501 (1997).
4. B. E. Gillman and S. D. Jacobs, *Appl. Opt.* **37**, 3498 (1998).
5. D. F. Edwards and P. P. Hed, *Appl. Opt.* **26**, 4670 (1987).
6. T. D. Fletcher, B. Dronen, F. T. Gobena, and E. Larson, "Fixed abrasive flat lapping with 3M trizact diamond tile abrasive pads," Presented at Optifab 2003, Rochester, New York, May 2003.
7. T. Fletcher, F. Gobena, & V. Romero, "Diamond fixed abrasive lapping of brittle substrates," Presented at the OSA Optical Fabrication & Testing Topical Meeting, Rochester, NY, November 11, 2004. <http://www.opticsinfobase.org/abstract.cfm?URI=OFT-2004-OMC1>
8. T. Bifano, Y. Yi, and W. K. Kahl, *Precis. Eng.* **16**, 109 (1994).
9. R. A. Jones, *Appl. Opt.* **16**, 218 (1977).
10. R. A. Jones, *Appl. Opt.* **18**, 1244 (1979).
11. W. Xu and Z. Xuejun, *Appl. Opt.* **48**, 904 (2009).
12. W. Xu, Z. Feng, and Z. Xuejun, *Opt. Precis. Eng.* **17**, 951 (2009).
13. Z. Xuejun, Z. Zhongyu, and L. Zhila, *Proc. SPIE* **6721**, 672109 (2007).
14. Z. Ligong and Z. Xuejun, *Proc. SPIE* **6288**, 62880N (2006).
15. Z. Wang, A. C. Bovik, H. R. Sheikh, and E. P. Simoncelli, *IEEE Trans. Image Process.* **14**, 600 (2004).